

Structure-based design of derivatives of tyropeptin A as the potent and selective inhibitors of mammalian 20S proteasome

Isao Momose,^{a,*} Yoji Umezawa,^b Sehei Hirose,^c
Hironobu Inuma^b and Daishiro Ikeda^a

^aNumazu Bio-Medical Research Institute, Microbial Chemistry Research Center, 18-24 Miyamoto,
Numazu City, Shizuoka 410-0301, Japan

^bMicrobial Chemistry Research Center, 3-14-23 Kamiosaki, Shinagawa-ku, Tokyo 141-0021, Japan

^cHiyoshi Medicinal Chemistry Research Institute, Microbial Chemistry Research Center, 3-34-17 Ida,
Nakahara-ku, Kawasaki-shi, Kanagawa, 211-0035, Japan

Received 12 January 2005; revised 3 February 2005; accepted 4 February 2005

Abstract—Tyropeptin A, a new potent proteasome inhibitor, was produced by *Kitasatospora* sp. MK993-dF2. To enhance the inhibitory potency of tyropeptin A, we constructed the structural model of tyropeptin A bound to the site responsible for the chymotrypsin-like activity of mammalian 20S proteasome. Based on these modeling experiments, we designed and synthesized several derivatives of tyropeptin A. Among them, the most potent compound, TP-104, exhibited a 20-fold enhancement in its inhibitory potency compared to tyropeptin A. Additionally, TP-110 specifically inhibited the chymotrypsin-like activity, but did not inhibit the PGPH and the trypsin-like activities.

© 2005 Elsevier Ltd. All rights reserved.

1. Introduction

The 26S proteasome consists of a central catalytic 20S proteasome and two terminal regulatory complexes, termed PA700 (also known as the 19S regulatory complex), which are attached to both ends of the central portion.^{1,2} The 20S proteasome is a large cylindrically-shaped complex composed of two copies each of seven distinct α - and seven distinct β -type subunits. All the subunits of yeast 20S proteasome have been cloned and sequenced, and can be grouped by sequence homology.³ The 20S proteasome possesses at least three distinctive protease activities of the post-glutamyl-peptide hydrolyzing (PGPH), trypsin-like and chymotrypsin-like activities, and were assigned to the active subunits of β 1, β 2, and β 5, respectively.

Proteasome degrades numerous regulatory proteins, such as cyclins, cyclin-dependent kinase inhibitors (e.g., p21 and p27), tumor suppressors (e.g., p53), and

the inhibitory proteins of the NF- κ B activation (e.g., I κ B- α), which are critical in tumor growth.^{4–7} Proteasome inhibitors can stabilize these regulatory proteins, and cause cell cycle arrest and apoptosis, and, as a result, can limit the tumor development. In 2003, PS-341, a dipeptide boronic acid proteasome inhibitor,^{8–10} was approved for cancer treatment for multiple myeloma patients. Therefore, the proteasome inhibitor is useful for the treatment of cancer.

Previously, we described the isolation and characterization of a new proteasome inhibitor, tyropeptin A, which was produced by *Kitasatospora* sp. MK993-dF2.^{11–13} The structure of tyropeptin A is isovaleryl-L-tyrosyl-L-valyl-DL-tyrosinal. Tyropeptin A significantly inhibits chymotrypsin-like activity in the three distinct protease activities of the 26S proteasome.

In the present study, to enhance the inhibitory potency of tyropeptin A, we constructed a structural model of tyropeptin A bound to the site responsible for the chymotrypsin-like activity of the mammalian 20S proteasome. We now report the utilization of the constructed model for the design of reasonable and effective modifications of tyropeptin A.

Keyword: Proteasome inhibitor.

*Corresponding author. Tel.: +81 55 924 0601; fax: +81 55 922 6888; e-mail: imomose@bikaken.or.jp

2. Model of tyropeptin A bound to the $\beta 5/\beta 6$ site of mammalian 20S proteasome

The crystal structure of the yeast 20S proteasome with a bound peptide aldehyde inhibitor, acetyl-L-leucyl-L-leucyl-L-norleucinal, revealed that the binding site responsible for the chymotrypsin-like activity of the 20S proteasome is formed by the association of the $\beta 5$ and $\beta 6$ subunits.¹⁴ Therefore, it is reasonable to conclude that the binding site responsible for the chymotrypsin-like activity of the mammalian 20S proteasome will also be formed by the association of the $\beta 5$ and $\beta 6$ subunits. Though the crystal structure of the human 20S proteasome has not yet been determined, the crystal structure of the mammalian 20S proteasome isolated from bovine was recently determined.^{15,16} The crystal structures and the amino acid sequences of the $\alpha 2$, $\beta 1$, $\beta 5$, $\beta 6$, and $\beta 7$ subunits of the bovine 20S proteasome are different from the *S. cerevisiae* 20S proteasome. Since the amino acid sequences of the $\beta 5$ and $\beta 6$ subunits of the bovine 20S proteasome show a 100% identity to those of the human 20S proteasome, the structural model of the $\beta 5/\beta 6$ site in the bovine proteasome adequately represents the $\beta 5/\beta 6$ site of the human proteasome. One possible binding model of tyropeptin A to the $\beta 5/\beta 6$ site of the mammalian 20S proteasome is shown in Figure 1.¹⁷ Figure 1A shows the expected binding mode of tyropeptin A to the $\beta 5/\beta 6$ site. It is conceivable that the aldehyde group of tyropeptin A forms a hemiacetal adduct with the catalytic Thr 1 residue of the $\beta 5$ subunit. Therefore, it is assumed that the tyrosinal, valine, and tyrosine resi-

dues of tyropeptin A mimic the role of the P1, P2, and P3 amino acids of the binding sites¹⁸ in the natural substrate of the proteasome, respectively. In addition, it is thought that residues Thr 21, Gly 47, and Ala 49 in the $\beta 5$ subunit and Asp 125 in the $\beta 6$ subunit are involved in the recognition of the peptide bonds of the substrate. Hence, assuming that tyropeptin A forms five β -sheet-like hydrogen bonds with the four residues, Thr 21, Gly 47, Ala 49, and Asp 125, and a hemiacetal adduct with the catalytic Thr 1 residue, we investigated the most favorable orientation of tyropeptin A in the $\beta 5/\beta 6$ binding site model using these hydrogen bonds and the adduct as modeling constraints. As a result, tyropeptin A nicely fits into the $\beta 5/\beta 6$ site (Fig. 1B). Figure 1B is an overview of the binding model of tyropeptin A bound to the $\beta 5/\beta 6$ site. Tyropeptin A was encircled by the association of the $\beta 5$ and $\beta 6$ subunits. In this binding model, four CH/ π interactions were observed (Fig. 1A). The CH/ π interaction is a hydrogen-bond-like weak attractive force observed between a CH hydrogen and π electron system, which was recently revealed to have a critical role in protein–ligand complexation and protein folding.¹⁹ The CH hydrogens of the side chains of Val 31, Lys 33, and Ala 49 in the $\beta 5$ subunit were able to form the CH/ π interactions with the π electron systems of the tyrosinal residue in tyropeptin A at the P1 position. The CH hydrogen of Ala 20 in the $\beta 5$ subunit was able to form the CH/ π interaction with the π electron systems of the tyrosine residue in tyropeptin A at the P3 position. In contrast, hydrogen bonds and/or CH/ π interactions between the *N*-terminal isovaleryl

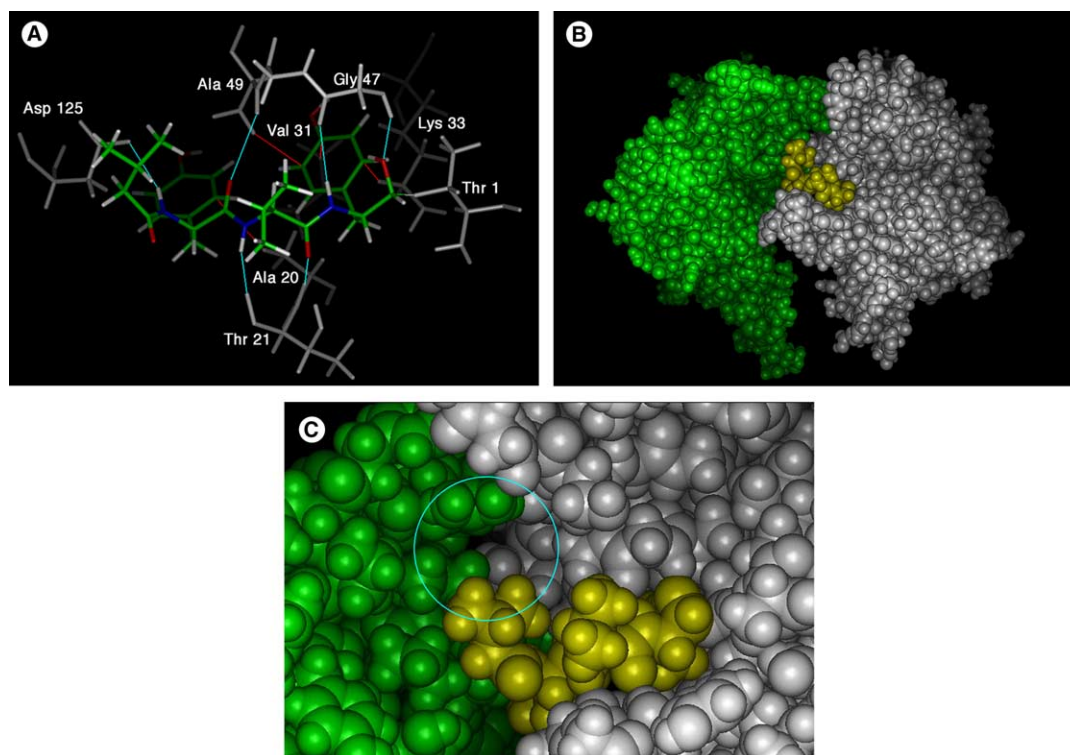


Figure 1. Binding model of tyropeptin A bound to the site responsible for the chymotrypsin-like activity of the 20S proteasome. (A) Expected binding mode of tyropeptin A to $\beta 5/\beta 6$ site. Tyropeptin A, atom colors; hydrogen bond, sky blue; CH/ π interaction, red; $\beta 5/\beta 6$ site, gray. (B) Overview of binding model of tyropeptin A bound to the $\beta 5/\beta 6$ site of the 20S proteasome. Subunit $\beta 5$, gray; subunit $\beta 6$, green; tyropeptin A, yellow. (C) Binding model of tyropeptin A in the $\beta 5/\beta 6$ site. Subunit $\beta 5$, gray; subunit $\beta 6$, green; tyropeptin A, yellow.

moiety of tyropeptin A and the 20S proteasome were not observed. This binding model suggested the presence of an open space in the vicinity of the *N*-terminal of tyropeptin A (Fig. 1C, sky blue circle). Since the isovaleeryl moiety in tyropeptin A only partially filled this area, we speculated that a compound capable of filling the open space may exhibit the enhanced inhibitory activity against the chymotrypsin-like activity of the 20S proteasome. Therefore, we designed tyropeptin A derivatives having a bulky *N*-terminal moiety.

3. Derivatives of tyropeptin A

According to the modeling studies mentioned above, we synthesized tyropeptin A derivatives modified at the *N*-terminal moiety and evaluated their inhibitory activities of 20S proteasome as shown in Table 1.²⁰ TP-104 exhibited a 20-fold inhibitory potency enhancement for the chymotrypsin-like activity compared to tyropeptin A. This increase in the inhibitory potency of TP-104 may come from the formation of hydrophobic or CH/ π interactions between the 1-naphthyl moiety and the $\beta 5/\beta 6$ site. To prove this hypothesis, we constructed a structural model of TP-104 bound to the $\beta 5/\beta 6$ site of the 20S proteasome (Fig. 2). Figure 2A shows the comparison with the three-dimensional structures of tyropeptin A and TP-104 at the $\beta 5/\beta 6$ site. As shown in Figure 2A, the 1-naphthyl moiety of TP-104 (right) well complements the shape of the open space in the vicinity of the *N*-terminal of tyropeptin A (left). Figure 2B shows the expected binding mode of TP-104 to the $\beta 5/\beta 6$ site. As expected, new interactions between the 1-naphthyl moiety and the $\beta 5/\beta 6$ site were observed. The CH hydrogens of the side chain of Ala 50 in the $\beta 5$ subunit and Val 127 in the $\beta 6$ subunit

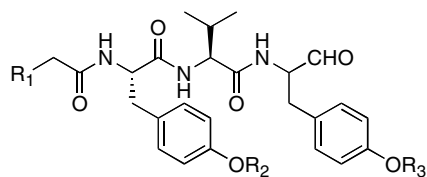
were able to form CH/ π interactions with the 1-naphthyl moiety of TP-104. Since new CH/ π interactions between the 1-naphthyl moiety of TP-104 and the $\beta 5/\beta 6$ site were formed, TP-104 had a very high affinity for the $\beta 5/\beta 6$ site. Therefore, TP-104 might be expected to show an increased inhibitory activity for the chymotrypsin-like activity of the 20S proteasome relative to tyropeptin A, which agrees with our experimental results.

The di-*O*-methyl derivative of TP-104, TP-110, inhibits the chymotrypsin-like activity with an IC_{50} value of 0.027 μM , but shows a marked decrease in its inhibitory activity for the trypsin-like activity (Table 1). TP-110 did not inhibit the trypsin-like and the PGPH activities even at the concentration of 100 μM , leading to an enhanced specificity for the chymotrypsin-like activity. The binding site of the trypsin-like activity is formed by the association of the $\beta 2$ and the $\beta 3$ subunits.¹⁶ The S1 and S3 pockets of the $\beta 2/\beta 3$ site were narrower than those of the $\beta 5/\beta 6$ site. Hence, the di-*O*-methyl derivative of TP-104, TP-110, may not optimally fit into the $\beta 2/\beta 3$ site. Therefore, TP-110 is a potent and selective inhibitor for the chymotrypsin-like activity of the mammalian 20S proteasome.

Our modeling studies of tyropeptin A bound to the 20S proteasome successfully designed the two compounds, TP-104 having a highly potent inhibitory activity against the 20S proteasome activities, and also TP-110, which specifically inhibits the chymotrypsin-like activity of the 20S proteasome. In this manner, our binding model of the bovine proteasome allowed us to rationally design potent inhibitors for the 20S proteasome. The evaluation of the anticancer activity of these compounds will be reported elsewhere.

Table 1. Inhibitory activities of the 20S proteasome by tyropeptin A derivatives

Compound	R_1	R_2	R_3	IC_{50} (μM)		
				Chymotrypsin-like activity	PGPH activity	Trypsin-like activity
Tyropeptin A	$CH(CH_3)_2$	H	H	0.14	68	5
TP-101	C_6H_{11}	H	H	0.033	17	3
TP-102	C_6H_5	H	H	0.027	16	2
TP-103	2-Naphthyl	H	H	0.014	4.7	0.7
TP-104	1-Naphthyl	H	H	0.007	4.9	1.2
TP-105	$CH_2(CH_2)_3CH_3$	H	H	0.037	20	2
TP-106	$CH(CH_3)_2$	H	CH_3	0.19	21	21
TP-107	$CH(CH_3)_2$	CH_3	CH_3	0.12	56	37
TP-108	1-Naphthyl	H	CH_3	0.018	38	6
TP-109	1-Naphthyl	CH_3	H	0.020	31	6
TP-110	1-Naphthyl	CH_3	CH_3	0.027	>100	>100
TP-111	$N(CH_3)_2$	H	H	1.2	>100	7.8
MG132				0.068	1.4	4.5



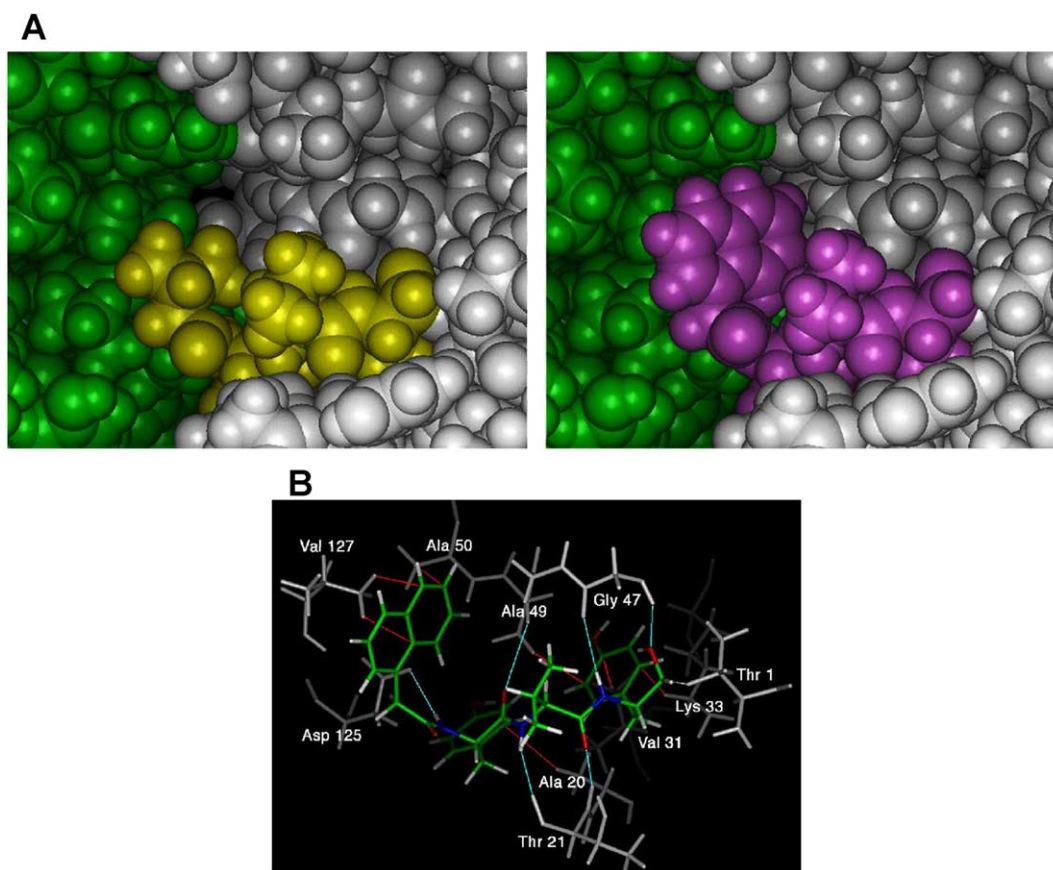


Figure 2. Binding model of TP-104 bound to the $\beta 5/\beta 6$ site of the 20S proteasome. (A) Comparison with structures of tyropeptin A and TP-104 in the $\beta 5/\beta 6$ site. Binding model of TP-104 in the $\beta 5/\beta 6$ site (right) compared to the tyropeptin A (left). Tyropeptin A is yellow and TP-104 is violet. (B) Expected binding mode of TP-104 to the $\beta 5/\beta 6$ site. Tyropeptin A atom colors; hydrogen bond, sky blue; CH/ π interaction, red; $\beta 5/\beta 6$, gray.

Acknowledgements

We would like to thank Dr. R. Sawa and Ms. Y. Kubota, Microbial Chemistry Research Center, for spectroscopic analysis, and Dr. T. Watanabe and Mr. M. Abe, Microbial Chemistry Research Institute, for useful discussions. This work was supported by the Public Trust Haraguchi Memorial Cancer Research Fund and a Grant-in-Aid for Scientific Research from the Japanese Ministry of Education, Culture, Sports, Science, and Technology (No 15790059).

References and notes

- Coux, O.; Tanaka, K.; Goldberg, A. L. *Annu. Rev. Biochem.* **1996**, *65*, 801.
- Voges, D.; Zwickl, P.; Baumeister, W. *Annu. Rev. Biochem.* **1999**, *68*, 1015.
- Heinemeyer, W.; Tröndle, N.; Albrecht, G.; Wolf, D. H. *Biochemistry* **1994**, *33*, 12229.
- Maki, C. G.; Howley, P. N. *Mol. Cell Biol.* **1997**, *17*, 355.
- Pagano, M.; Tam, S. W.; Theodoras, A. M.; Beer-Romero, P.; Del Sal, G.; Chau, V.; Yew, P. R.; Draetta, G. F.; Rolfe, M. *Science* **1995**, *269*, 682.
- Ciechanover, A.; DiGiuseppe, J. A.; Bercovich, B.; Orian, A.; Richter, J. D.; Schwartz, A. L.; Brodeur, G. M. *Proc. Natl. Acad. Sci. U.S.A.* **1991**, *88*, 139.
- Palombella, V. J.; Rando, O. J.; Goldberg, A. L.; Maniatis, T. *Cell* **1994**, *78*, 773.
- Adams, J.; Behnke, M.; Chen, S.; Cruickshank, A. A.; Dick, L. R.; Grenier, L.; Klunder, J. M.; Ma, Y.-T.; Plamonda, L.; Stein, R. L. *Bioorg. Med. Chem. Lett.* **1998**, *8*, 333.
- Adams, J.; Palombella, V. J.; Sausville, E. A.; Johnson, J.; Destree, A.; Lazarus, D. D.; Maas, J.; Pien, C. S.; Prakash, S.; Elliott, P. *J. Cancer Res.* **1999**, *59*, 2615.
- Richardson, P. G.; Barlogie, B.; Berenson, J.; Singhal, S.; Jagannath, S.; Irwin, D.; Rajkumar, S. V.; Srkalovic, G.; Alsina, M.; Alexanian, R.; Siegel, D.; Orlowski, R. Z.; Kuter, D.; Limentani, S. A.; Lee, S.; Hideshima, T.; Esseltine, D. L.; Kauffman, M.; Adams, J.; Schenkein, D. P.; Anderson, K. C. *New Engl. J. Med.* **2003**, *348*, 2609.
- Momose, I.; Sekizawa, R.; Hashizume, H.; Kinoshita, N.; Homma, Y.; Hamada, M.; Iinuma, H.; Takeuchi, T. *J. Antibiot.* **2001**, *54*, 997.
- Momose, I.; Sekizawa, R.; Hirosawa, S.; Ikeda, D.; Naganawa, H.; Iinuma, H.; Takeuchi, T. *J. Antibiot.* **2001**, *54*, 1004.
- Momose, I.; Sekizawa, R.; Iinuma, H.; Takeuchi, T. *Biosci. Biotechnol. Biochem.* **2002**, *54*, 1004.
- Groll, M.; Ditzel, L.; Löwe, J.; Stock, D.; Bochtler, M.; Bartunik, H. D.; Huber, R. *Nature* **1997**, *386*, 463.
- Unno, M.; Mizushima, T.; Morimoto, Y.; Tomisugi, Y.; Tanaka, K.; Yasuoka, N.; Tsukihara, T. *J. Biochem. (Tokyo)* **2002**, *131*, 171.
- Unno, M.; Mizushima, T.; Morimoto, Y.; Tomisugi, Y.; Tanaka, K.; Yasuoka, N.; Tsukihara, T. *Structure* **2002**, *10*, 609.

17. X-ray crystal structure data of the bovine 20S proteasome were taken from the Protein Data Bank with the accession code 1IRU. The complex model structure was optimized with the Discover program of Insight II (Accelrys). The CH/ π interactions were detected by the CHPI program (Nishio, M.; Hirota, M.; Umezawa, Y. *The CH/ π Interaction. Evidence, Nature, and Consequences*; Wiley-VCH: New York, 1998). This program was written in order to search for the short contacts between the CH groups and π system in protein structures, and is able to detect XH/ π interactions (X = C, N, O, and S) based on bond length and angle parameters.
18. Schechter, I.; Berger, A. *Biochem. Biophys. Res. Commun.* **1967**, 27, 157.
19. Umezawa, Y.; Nishio, M. *Bioorg. Med. Chem.* **1998**, 6, 493.
20. The chymotrypsin-like, trypsin-like and PGPH activities of the 20S proteasome were measured using fluorogenic substrates as previously described.¹¹ 20S proteasome was prepared from human leukemia HL-60 cells.